

Production of Nanocomposites of PET-Montmorillonite Clay by an Extrusion Process

A. Sanchez-Solis*, A. Garcia-Rejon†, O. Manero

Instituto de Investigaciones en Materiales. Universidad Nacional Autónoma de México. Apartado Postal 70-360. Coyoacán, 04510. México, D.F.
Email:sancheza@servidor.unam.mx

†Industrial Materials Institute. National Research Council of Canada. 75 de Mortagne J4B 6Y4. Boucherville, Quebec. Canada

Summary: Polyethylene terephthalate (PET) was mixed by extrusion with clay (montmorillonite) to produce nanocomposites. Additives (pentaerythritol and maleic anhydride) were added to induce compatibility between the particles and the matrix. Thermal, mechanical and rheological properties of the nanocomposites were evaluated. The nanocomposites with additives presented improved mechanical strength. In shear, the viscoelastic properties decrease with rising particle concentration and additives content. The resulting new materiales present processing advantages and potential improvements in performance.

Introduction

Polymeric nanocomposites are a class of relatively new materials with ample potential applications. Products with commercial applications appeared during the last decade^[1], and much industrial and academic interest have produced. Reports on the manufacture of nanocomposites include those made with polyamides^[2-5], polyolefines^[6-9], polystyrene and polystyrene copolymers^[10-11], ethylene vinyl alcohol^[12-15], acrylics^[16-18], polyesters^[19-20], polycarbonate^[21-22], liquid crystalline polymers^[23-26], fluoropolymers^[27-29], thermoset resins^[30-32], polyurethanes^[33-38], ethylene-propylene oxide^[39], vinyl carbazole^[40-41], polydiacetylene^[42], and polyimides^[43], among others.

Generally, polymer nanocomposites can be obtained through two routes: the first one is the polymerization of monomers in contact with the exfoliated clay, and the second one uses existing transformation processes to produce nanocomposites, as for example, by a reactive extrusion. There are, however, problems present due to the lack of affinity of the clay-polymer system because of the hydrophilic character of the particles. It is then necessary to treat the clay chemically to increase its affinity with the polymer matrix. This constitutes another whole area of research in the nanocomposites production.

The mixing of the nano-particle with the polymer requires an intercalation process of the macromolecule into the clay galleries gap. This is a diffusion-controlled process which requires long times of contact between the polymer and the clay under the pressure produced inside the extruder. The intercalation process leads to the exfoliation of the clay. However, low screw speeds and long residence times in the extruder may cause polymer degradation. To avoid such problem that would enable the complete clay exfoliation, it would be necessary to change the screw configuration or to consider the chemical modification of the clay. Moreover, the clay exfoliation is not a sufficient condition to obtain optimum systems. The problem of compatibility of the clay-polymer matrix is an outstanding one, and the thermodynamic processes involved in the synthesis of these materials^[44-45], constitute areas which are currently under investigation.

The macroscopic effects of the integration of nanoparticles to the polymer matrix are quite remarkable. For example, the barrier properties of the new systems are enhanced, because the diffusion of gas molecules through the material is largely retarded. A lower permeability of O₂ is obtained without substantially modifying the production method of films, containers, bottles, etc. Oxygen permeability decreases drastically with nanoparticle concentration.

In this work, the production process of a polymeric nanocomposite made of polyethylene terephthalate (PET) and a commercial clay (montmorillonite) is described. The clay is chemically modified with a quaternary ammonium salt, using maleic anhydride (MAH) and pentaerythritol (PENTA) as compatibilizing agents. Thermal, mechanical and rheological properties of PET are substantially modified. In addition, the viscoelastic behavior of the new systems is discussed.

Experimental Procedure

Materials

PET Eastapack 9921 from Eastman Chemical had a density of 1.40 g/cm³ and melting point of 269°C. A glass transition temperature (T_g) of 61.2°C was determined. MAH and PENTA are analytic reagents from Aldrich with melting points of 55°C and 192.8°C, respectively. These reagents were used as received. Thermal properties were determined by differential scanning calorimetry (DSC) with a heating speed of 20°C/min under nitrogen atmosphere. No additives to prevent oxidation were used in the formulations. Clay montmorillonite (Cloisite 15A) from Southern Clay Co., is a natural clay modified with a quaternary ammonium salt, had a density of 1.66g/cm³ and a ionic interchange capacity of 125 meq/100g.

Equipment

Blends were made in a co-rotating twin-screw extruder (Werner & Pfleiderer ZSK30) equipped with a volumetric band feeder under nitrogen atmosphere to prevent moisture absorption. Moisture determinations were carried out in a Moisture Analyzer Omnimark Mark2. Interlayer distance among clay platelets was determined in a Bruker-AXSD8-Advance Diffractometer with a wavelength of $\text{CuK}\alpha = 1.5418 \text{ \AA}$ at 35kv and 30 mA with scanning speed of $1^\circ 2\theta/\text{min}$. Bottles were made in an injection-stretch blow-molding machine AOKI on one step with a temperature profile of 275°C at the feeder and 320°C at the injection nozzle, with perform temperature of 112°C and blow mold temperature of 16°C . Determination of the rheological properties was carried out in a TA-Instruments AR 1000-N controlled stress rheometer with parallel plates of 25 mm diameter.

Results

Thermal Properties

Clay concentrations larger than 2 wt.% cause a decrease in the glass transition temperature (T_g), and therefore only clay concentrations of 1% and 2% were considered. Raw materials were previously mixed before placing them in the extruder feeder. Extruded threads were cooled and cut into pellets of 5 mm length. Thermal properties of blends made with PET, clay, MAH and PENTA are shown in figures (1) and (2). Crystallinity of the samples was calculated using the relation $\%crystallinity = (\Delta H_m / \Delta H_m^0) * 100$ where ΔH_m^0 is the theoretical melt enthalpy of the PET crystal (117.6 J/g) and ΔH_m is the sample enthalpy⁴⁷.

Concentrations of MAH and PENTA used were 0.12% and 0.03 %, respectively, for a clay content of 1 wt%. They were increased to 0.24% and 0.06 %, respectively, for clay a content of 2%. The large additive concentration systems include concentrations of 0.24% and 0.06 % when the clay content is 1%, and 0.48% and 0.12 %, respectively, for a clay content of 2%.

Figure (1) shows that the crystallization temperature diminishes with clay concentration for the system with no additives. As the clay-quaternary ammonium salt, MAH and PENTA are added; the crystallization temperature (T_c) diminishes even more with clay concentration (the melting temperature, T_m , remains practically constant). For the system with large MAH and PENTA concentrations, the decrease in the crystallization temperature is much smaller than that observed in the system with no additives and in the system with small concentrations of

additives.

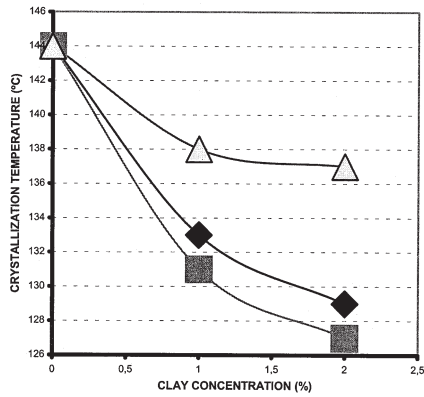


Figure 1. Crystallization temperature as a function of clay concentration for the system without additives (◆), with MAH and PENTA (small concentrations) (■) and with MAH and PENTA (large concentrations) (▲)

As observed in figure (2), for increasing clay concentration larger crystallinity is attained, since clay particles may act as nucleation agents. The system with large additive concentrations shows a remarkable increase of the crystallinity with clay concentration. In addition, ΔH_m increases with clay content, suggesting that a large amount of energy is necessary to melt the crystals.

When nanocomposites are produced by polymerization *in situ*, it was found^[19] that T_c and T_m decrease slightly as a function of clay concentration (5%), but the melting enthalpy decreases with clay concentration. These discrepancies arise because the different production procedures.

Clay Exfoliation

The clay interlayer distance (d_{001} , referred to the plane 001) was determined by X-rays diffraction. The diffraction area is located at low angles, such as 2θ (the diffraction position) is smaller than 10° , which corresponds to an interlayer distance $> 8.84 \text{ \AA}$ (according to the Bragg equation: $2d_{001} \sin \theta = \lambda$). λ is the wavelength of radiation (1.5418 \AA). The clay has an interlayer distance equal to 31.5 \AA . All nanocomposites analyzed present similar values, which means that none of the samples reached a complete clay exfoliation. It was concluded

that it is necessary to use different screw configurations to produce exfoliation.

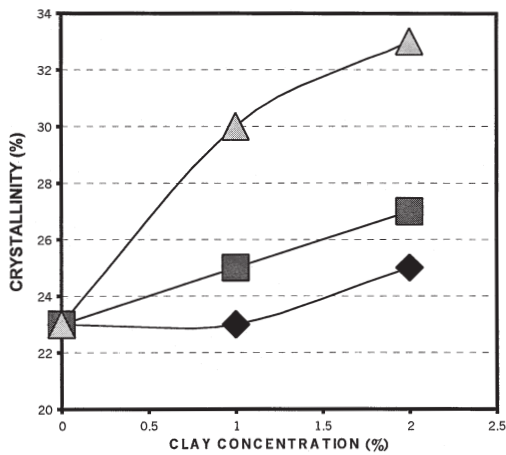


Figure 2. Crystallinity versus clay concentration for the three systems shown in figure (1)

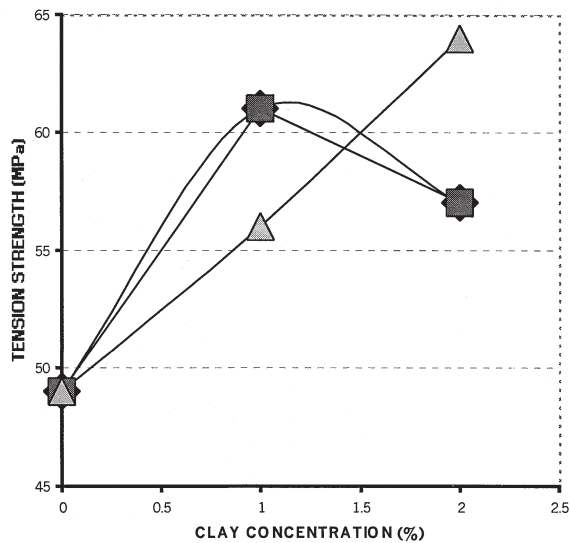


Figure 3. Tension strength as a function of clay concentration, for same systems shown in figure (1). Temperature of the test is 270°C

Tensile Mechanical Properties

Tensile mechanical properties were performed on specimens cut from bottles made by the injection-stretch blow-molding process. PET was crystallized during 48 hours at 130°C

previously to processing, to avoid possible jamming in the machine due to the amorphous content of the material. The bottles produced from PET-clay are transparent with slight coloring (white to brown). It is necessary to mention that the mechanical properties were measured on systems with the same thermomechanical history, and therefore they have similar degrees of degradation due to processing.

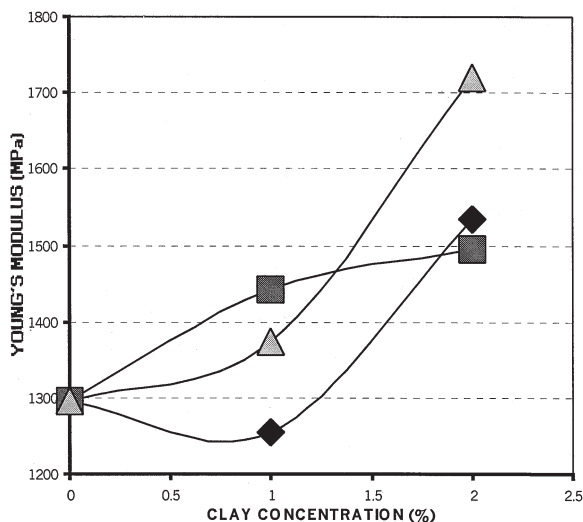


Figure 4. Variation of the Young modulus with clay concentration for same systems of previous figures. $T = 270^{\circ}\text{C}$

In general, it is observed that mechanical properties of nanocomposites are largely improved when the clay particles are totally exfoliated and good phase affinity is attained. The mechanism by which these improvements are obtained considers the absorption of macromolecular layers on the clay platelet surface. As a consequence, the diffusion of molecules is impeded and retarded, and hence the material acquires additional crystallinity. This effect produces increases in the material strength and modulus.

However, it is not necessary to obtain a complete exfoliation of the particles, since non-exfoliated nanocomposites may present improvements in mechanical properties as well. For instance, in this study, complete clay exfoliation was not attained, but the compatibility and particle dispersion reached through the action of the additives lead to an increase in the mechanical properties, up to 30% and 32% in strength and modulus, respectively (see figures

3 and 4). In figure (3), the tension strength presents a maximum in PET with 1% clay concentration, in systems with no additives or with small additive concentration. For larger additives concentration, there is a continuous rise in the strength up to 2 % clay content. A similar increase in the Young's modulus is also obtained in the system with the larger additive concentration, as shown in figure (4). The mechanism by which this improvement has been reached is not completely clear, because the lack of understanding on the compatibilizers (additives) action, and so additional work is necessary.

Rheological Properties

As in the mechanical properties, the rheological properties were measured on systems with the same thermorheological history, so the measurements shown correspond to systems with same degradation due to processing. The viscosity variation with shear rate for processed PET, PET with clay and PET with clay plus additives is shown in figure (5). In addition, in figure (6) the zero shear-rate viscosity for the seven systems of figure (5) is plotted with clay concentration.

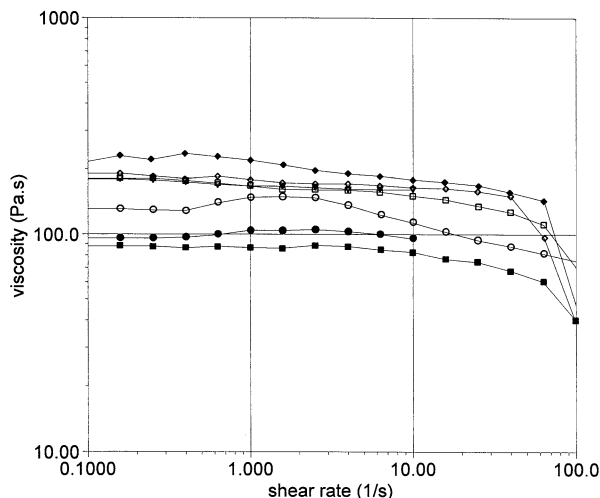


Figure 5. The shear viscosity is plotted versus shear rate for various systems: \blacklozenge processed PET, ∇ 1% clay without additives, \square 1% clay with MAH and PENTA, \diamond 1% clay with high MAH and PENTA contents, \circ 2% clay without additives, \bullet 2% clay with MAH and PENTA, $+$ 2% clay with high MAH and PENTA contents. $T = 270^{\circ}\text{C}$

The basic behavior shows a near-linear decrease of the zero shear-rate viscosity with clay

concentration. The viscosity lowers to values less than a half of the PET viscosity for 2% clay content. Additives promote an even lower viscosity at high clay contents, but they do not have any substantial effect at low clay contents.

As is well known in injection processes, smaller viscosities of the polymer in the melt state results in better filling of the mold cavities. On the other hand, in extrusion processes, the loss of melt strength caused by lower viscosity, requires that the material should be processed at lower temperatures to preserve consistency and to avoid sagging, which means smaller thermal degradation.

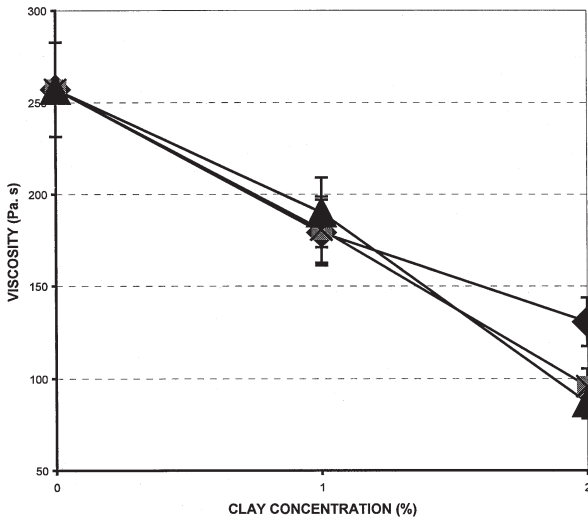


Figure 6. Zero shear-rate viscosity versus clay concentration. Symbols are the same as in figure 1

The reduction of the complex viscosity with clay concentration and the effect of the additives on the viscosity follow the same tendency to that observed in the shear viscosity, as shown in figure (7). However, there are substantial differences for shear rates higher than 10 s^{-1} , specially when the clay content is 2%. Comparison of figures (5) and (7) illustrates that for high clay contents, particle alignment with the flow induce the shear thinning observed in the high shear rate region. On the other hand, at low shear rates particles are not aligned and a region of shear thickening is observed in the system with 2% clay content without additives. The shear thickening effect decreases with addition of additives, which clearly reflects the consequences of increased compatibility of the particles with the matrix. The onset point for shear-thinning, which is closely related to the relaxation time in shear, is shifted to lower

deformation rates with respect to those of the complex viscosity. This indicates that as the clay content increases, the shear viscosity is governed by a relaxation time which is larger than that which governs the complex viscosity. This increase in the characteristic time of the system is ascribed to the effect of the particles on the flow, and this effect is larger with increasing compatibility caused by rising additive concentration.

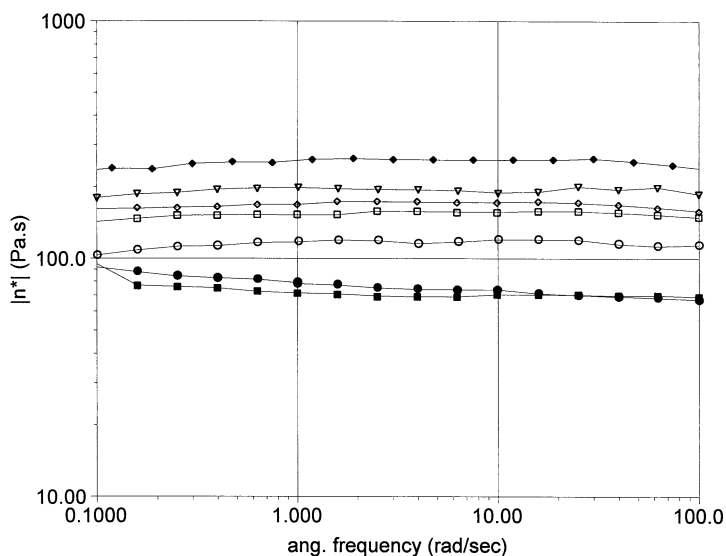


Figure 7. The complex viscosity is plotted versus angular frequency for the seven systems shown in figure 5. $T = 270^{\circ}\text{C}$

To assess the effect of increasing clay and compatibilizing agent concentration on the linear viscoelastic properties of the systems, the elastic modulus (G') is shown as a function of frequency (figure 8) and also as a function of clay concentration (figure 9) at a fixed frequency (100 s^{-1}). Temperature of the tests was set at 270°C .

The variation of the elastic modulus with frequency indicates that for large frequencies, the overall effect of the addition of clay is similar to that observed in the shear viscosity, i.e., a continuous decrease of the viscoelastic properties with clay concentration. The decrease is larger when additives are added. On the other hand, at low frequencies the modulus does not approach a slope of two, and hence additional relaxation modes exist besides the main relaxation mechanism. The effect of high additive contents is more evident at low frequencies,

where the systems depict higher modulus. In this case compatibility is reflected in the widening of the relaxation spectrum of the polymer due to the presence of the particles.

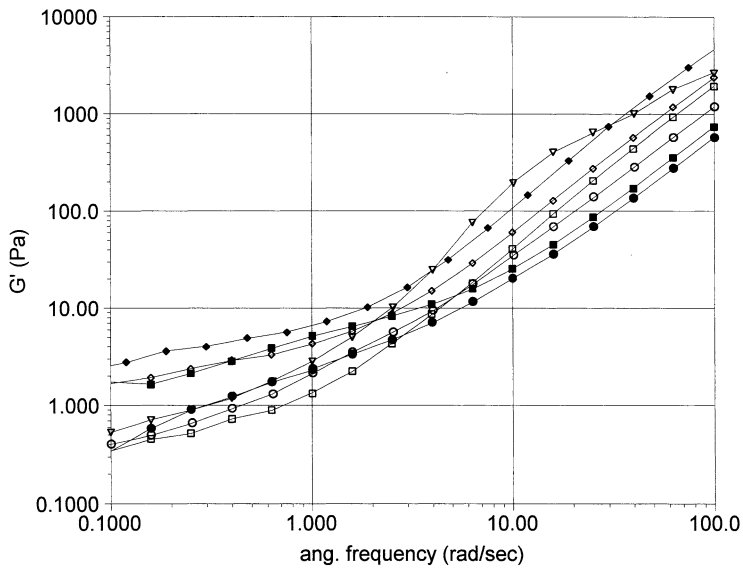


Figure 8. Storage modulus versus angular frequency for the seven systems indicated in figure (5). $T = 270^{\circ}\text{C}$

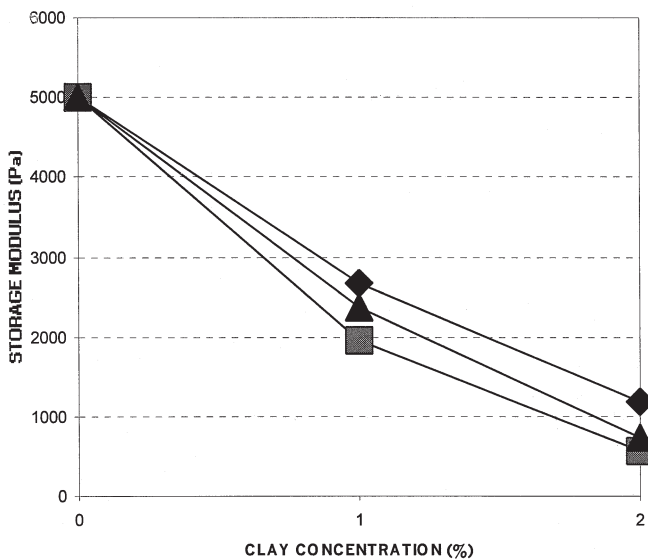


Figure 9. Storage modulus versus clay concentration. Symbols are the same as in figure 1

Discussion and Conclusions

The addition of clay nanoparticles to polyethylene terephthalate (PET) to produce a nanocomposite, affects the thermal properties of PET, such as the crystallization temperature. The additives used here (MAH and PENTA) produce an increased crystallinity with higher modulus and material strength. These nanocomposites present smaller shear viscosity and lower magnitudes of the linear viscoelastic properties than those of PET. The viscoelastic properties are affected strongly by the interaction between polymer and clay particles, due to increasing polarity.

Observation of the results of the mechanical and rheological properties of the systems analyzed in this study, it is remarkable that while in simple shear and oscillatory flow the rheological properties show a substantial decrease with increasing particle concentration (in the systems with large additives concentration), in extensional flow the mechanical properties and materials strength increase. This effect reflects, on the one hand, a diminishing particle-matrix interaction as the clay concentrations rises. On the other hand, the compatibility of the particles with the matrix induced by the additives and the increase in crystallinity, leads to materials with increasing strength and modulus as the clay concentration rises.

These results show the advantages of nanocomposites in the processing operations and final properties of these new materials. When polymeric nanocomposites are undergoing a deformation by shear in the processing operation, the modified rheological behavior due to the presence of the particles induce better surface properties with smaller shrinkages when the polymer solidifies inside the mold (in injection-molding) or outside the die (in extrusion). These results show potential advantages in processing and performance of these new materials.

Acknowledgements

Authors wish to thank C. Granpre and Y. Zimmard for their collaboration in the injection blow-molding and extrusion work, respectively. Also, we thank Dr. M. Estrada for the X-Ray measurements, Dr. A. Maciel for the mechanical measurements and Mr. F. Calderas for the rheometric work. Support from project G-27837U (CONACYT) is also acknowledged.

- [1] Y. Kojima, A. Usuki, M. Kawasumi, A. Okada, Y. Fukushima, T. Kurauchi, O. Kamigaito. *J. Mater. Res.* **1993**, 8, 1185.
- [2] A. Okada, A. Usuki. *Mater. Sci. Eng.* **1995**, C3, 109.
- [3] M. K. Akkapeddi. *Polym. Comp.* **2000**, 21(4), 576.
- [4] L. Liu, Z. Qi, X. Zhu. *J. Appl. Polym. Sci.* **1999**, 71(7), 1133.
- [5] L. P. Cheng, D.J. Lin, K.C. Yang. *J. Membranes. Sci.* **2000**, 172, 157.
- [6] M. Kawasumi, N. Hasegawa, M. Kato, A. Usuki, A. Okada. *Macromolecules.* **1997**, 30, 6333.
- [7] M. Kato, A. Usuki, A. Okada. *J. Appl. Polym. Sci.* **1997**, 66(9), 1781.
- [8] J. Heinemann, P. Reichert, R. Thomann, R. Mulhaupt. *Macromol. Rapid. Commun.* **1999**, 20(8), 423.
- [9] H. G. Jeong, H.T. Jung, S.W. Lee, S.D. Hudson. *Polym. Bull.* **1998**, 41(1), 107.
- [10] M. H. Noh, D. C. Lee. *J. Appl. Polym. Sci.* **1999**, 74(12), 2811.
- [11] X. Fu, S. Qutubuddin. *Polymer.* **2001**, 42(2), 807.
- [12] P. B. Messersmith, E. P. Giannelis. *Chem. Mater.* **1993**, 5(8), 1064.
- [13] R. A. Vaia, S. Vasudevan, W. Krawiec, L. G. Scanlon, E. P. Giannelis. *Adv. Mater.-Weinheim.* **1995**, 7(2), 154.
- [14] R. Levy, C.W. Francis. *J. Coll. Inter. Sci.* **1975**, 50(3), 442.
- [15] D.J. Greenland. *J. Collo. Sci.* **1963**, 18, 647.
- [16] C.D. Muzny, B.D. Butler, H.J.M. Hanley, F. Tsvetkov, D.G. Peiffer. *Mater. Letters.* **1996**, 28(4), 379.
- [17] M. Okamoto, S. Morita, H. Taguchi, Y. H. Kim, T. Kotaka, H. Tateyama. *Polymer.* **2000**, 41(10), 3887.
- [18] F. Dietsche, R. Mulhaupt. *Polym. Bull.* **1999**, 43(4-5), 395.
- [19] Y. Ke, C. Long, Z. Qi. *J. Appl. Polym. Sci.* **1999**, 71(7), 1139.
- [20] J. C. Matayabas, S. R. Turner, B. J. Sublett, G. W. Connell, J. W. Gilmer, R. B. Barbee. Patent # 6084019 USA, 2000.
- [21] N. R. Rosenquist, K. F. Miller. Patent # 4786710 USA, 1988.
- [22] X. Huang, S. Lewis, W. J. Brittain, R. A. Vaia. *Macromolecules.* **2000**, 33(6), 2000.
- [23] J. Heinemann, P. Reichert, R. Thomann, R. Mulhaupt. *Macromol. Rapid. Commun.* **1999**, 20, 423.
- [24] E. P. Giannelis. *Adv. Mater.* **1996**, 8(1), 29.
- [25] P. Aranda, E. Ruiz-Hitzky. *Appl. Clay. Sci.* **1999**, 15, 119.
- [26] A. Usuki, A. Koiwai, Y. Kojima, M. Kawasumi, A. Okada, T. Kurauchi, O. Kamigaito. *J. Appl. Polym. Sci.* **1995**, 15, 119.
- [27] M. J. Michalczyk, K. G. Sharp, C. W. Stewart. Patent # 5726247 USA, 1998.
- [28] S. Badesha, A. Henry, J. Maliborski, E. Clifford. Patent # 5840796 USA, 1998.
- [29] M. W. Ellsworth. Patent # 5962553 USA, 1999.
- [30] M. Wang, T. Pinnavaia. *Chem. Mater.* **1994**, 6(4), 468.
- [31] C. Zilg, R. Mulhaupt, J. Finter. *Macromol. Chem. Phys.* **1999**, 200(3), 661.
- [32] X. Kornmann, L. A. Berglund, J. Sterte, E. P. Giannelis. *Polym. Eng. Sci.* **1998**, 38(8), 1351.
- [33] L. Chen, K. Liu, C.Z. Yang. *Polym. Bull.* **1996**, 37(3), 377.
- [34] T. Hirai, M. Miyamoto, I. Komasaawa. *J. Mater. Chem.* **1999**, 9(6) 1217.
- [35] Z. Wang, T. J. Pinnavaia. *Chem. Mater.* **1998**, 10(12), 3769.
- [36] C. Zilg, R. Thomann, R. Mulhaupt, J. Finter. *Adv. Mater.* **1999**, 11(1), 49.
- [37] T.K. Chen, Y.I. Tien, K.H. Wei. *J. Appl. Polym. Sci.* **1999**, Part A: Polym. Chem. 37(13), 2225.
- [38] T. K. Chen, Y.I. Tien, K.H. Wei. *Polymer.* **2000**, 41(4), 1345.
- [39] G. Spenleuhauer, D. Bazile, M. Veillard, C. Prud'Homme, J. P. Michalon. Patent # 5766635 USA, 1998.
- [40] M. Biswas, S. Sinha Ray. *Polymer.* **1998**, 39(25), 6423.
- [41] S. Sinha Ray, M. Biswas. *J. Appl. Polym. Sci.* **1999**, 73(14), 2971.
- [42] T. Srikinirin, A. Moet, J. B. Lando. *Polym. Adv. Tech.* **1998**, 9(8), 491.
- [43] H. Tyan, Y. Liu, K. Wei. *Chem. Mater.* **1999**, 11(7), 1942.
- [44] R. A. Vaia, E. P. Giannelis. *Macromolecules.* **1997**, 30, 7990.
- [45] R. A. Vaia, E. P. Giannelis. *Macromolecules.* **1997**, 30, 8000.
- [46] L. Quintanilla, M. Alonso, J. Rodriguez, M. Pastor. *J. Appl. Polym. Sci.* **1996**, 59, 769.